Mechanical Engineering Advances 2025, 3(2), 2052.
https://doi.org/10.59400/mea2052

Article

Two-phase heat conductors for passive thermal regulation systems of electric vehicles

Leonard Vasiliev*, Alexander Zhuravlyov, Dmitry Sadchenko

Porous Media Laboratory, A.V. Luikov Heat and Mass Transfer Institute of the National Academy of Science of Belarus, Minsk 220072, Republic of Belarus
*** Corresponding author:** Leonard Vasiliev, leonard_vasiliev@rambler.ru

CITATION

Vasiliev L, Zhuravlyov A, Sadchenko D. Two-phase heat conductors for passive thermal regulation systems of electric vehicles. Mechanical Engineering Advances. 2025; 3(2): 2052.
https://doi.org/10.59400/mea2052

ARTICLE INFO

Received: 7 February 2025
Accepted: 27 February 2025
Available online: 9 April 2025

COPYRIGHT

Copyright © 2025 by author(s). *Mechanical Engineering Advances* is published by Academic Publishing Pte. Ltd. This work is licensed under the Creative Commons Attribution (CC BY) license.
https://creativecommons.org/licenses/by/4.0/

Abstract: Due to the growing demands for a better environment, great efforts are currently being made in the world to create and improve electric and hybrid vehicles. Heat-loaded equipment of electric transport requires efficient cooling systems. A loop thermosyphon made of aluminum, having two flat multi-channel evaporators and one condenser for cooling electronic components, is developed and tested with acetone as the working fluid. The procedure and results of an experimental study of the characteristics of a thermosyphon are described. The evaporators are supplied with a heat load of varying power; the absorbed heat is dissipated by the condenser. The working fluid is acetone. The influence of thermal load and volume of working fluid on the thermal resistance of a thermosyphon and its components was determined and investigated. The lowest evaporator thermal resistance is 0.15 K/W for the heat load range 30–60 W. The thermosyphon operates stably in a wide range of thermal loads and quickly responds to their changes.

Keywords: electric and hybrid vehicles; thermosyphon; double evaporator loop thermosyphon; passive thermal regulation; multi-channel evaporators; green technologies in transport

1. Introduction

Reducing the consumption of hydrocarbon fuels and improving the environmental situation are urgent tasks. Vehicle emissions are a very serious problem. Internal combustion engines (ICE) emit carbon dioxide CO_2, carbon monoxide CO, nitrogen oxides NO_x and other harmful substances into the atmosphere. While industry, the electricity grid and other polluters have cut fossil CO_2 over the past 30 years, fossil CO_2 from transport continues to increase. For example, in the UK alone, the number of cars has increased to 40.7 million units in 2023, while their weight has doubled and they require twice as much fuel since 1980 [1]. According to a study [2], global aviation accounts for approximately 2.1% of anthropogenic CO_2 emissions. If no effective measures are taken, then by 2050 CO_2 emissions from air transport will reach 23% of all transport emissions and 5% (15% in the worst-case scenario) of total greenhouse gas emissions. In this regard, great importance is attached to the creation and improvement of hybrid and electric technologies in transport [3,4].

According to some estimates, replacing internal combustion engine vehicles with electric vehicles could reduce greenhouse gas emissions by 20% and by 40% when generating electricity from renewable sources [5,6]. The importance of the above-mentioned problems and the prospects of the chosen strategy are evidenced by the fact that work on the creation of electric and hybrid power plants is actively carried out not

only in the automobile industry but also in the aircraft industry, where the requirements for reliability, safety, and efficiency (including weight) are extremely strict. In aviation, one of the promising solutions to this global problem is electric aircraft. Replacing aircraft with internal combustion engines with electric ones will ensure a significant reduction in greenhouse gas emissions [7–9].

Modern means of transport (electric cars, electric aircraft, hybrid vehicles, etc.) are characterized by designs that operate under conditions of intense, often extreme, thermal effects. Electric and hybrid vehicles require efficient cooling due to the presence of a significant number of heat-generating components, including the powertrain, navigation electronics, battery, headlights, etc. (**Figures 1** and **2**).

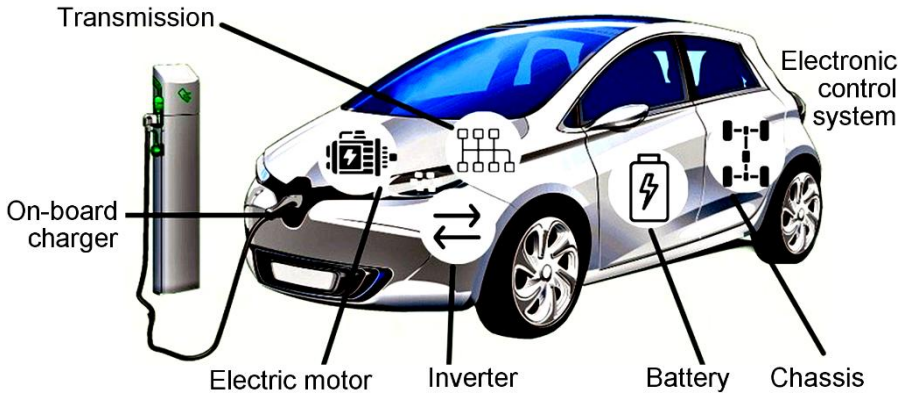

Figure 1. Heat-loaded elements of an electric vehicle.

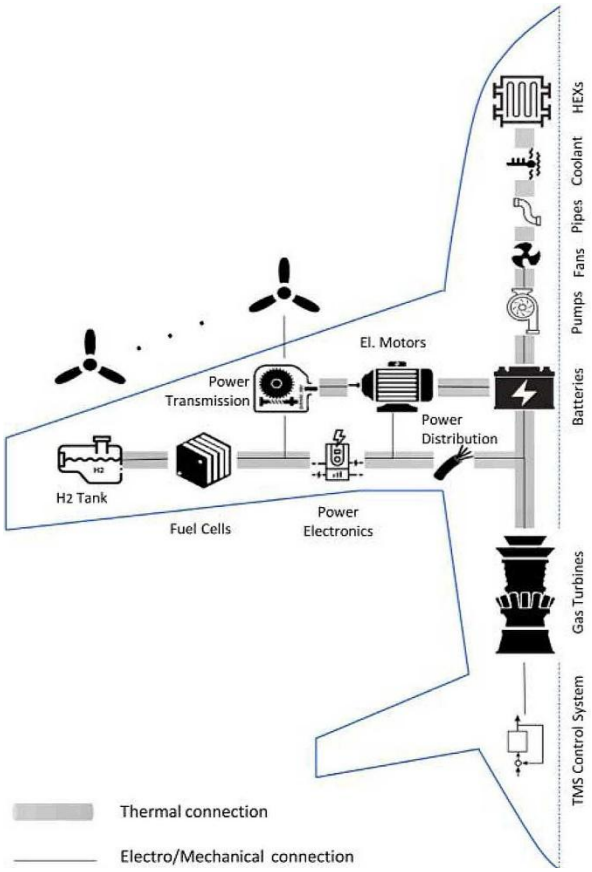

Figure 2. Main subsystems and components of the thermal control system in a general-purpose hybrid electric propulsion aircraft [10].

For thermal regulation of heat-generating objects of electric transport, various systems can be used: air, liquid, with the use of phase-changing materials, thermoelectric, immersion in boiling liquid. The air free-convection system is simple, relatively cheap, and electrically safe, but due to the low heat capacity and thermal conductivity of air, it is effective when intensive blowing of radiators is possible. Liquid cooling is more effective but requires a coolant reservoir and an energy-consuming pumping system. Phase-changing materials maintain a constant temperature of the object, are not energy-consuming, allow for the possibility of leakage of molten material, and are limited by the available amount of latent heat. energy-consuming pumping system. Thermoelectric coolers based on the Peltier effect are capable of precisely controlling the temperature of an object, are reliable, silent, compact, lightweight, and easy to operate, but are less efficient than other systems.

The problem of removing excess heat from heat-generating electronic equipment can be successfully solved using heat pipes and thermosyphons—highly heat-conducting two-phase heat conductors with an evaporation-condensation cycle, in which heat is transferred by transferring the latent heat of evaporation. These devices are autonomous and silent, and their operation does not require energy consumption, which is very important for wireless electric transport. They can absorb heat from the object being cooled, transfer it outside the volume filled with equipment, and then transfer it to the cooling liquid or air. Heat pipes and thermosyphons are easy to operate, have no mechanical moving parts, do not require energy consumption or maintenance, and can provide heat exchange between the surface of the cooled object and the external environment with virtually no heat loss. They can be used to ensure efficient heat removal from a heat-loaded component.

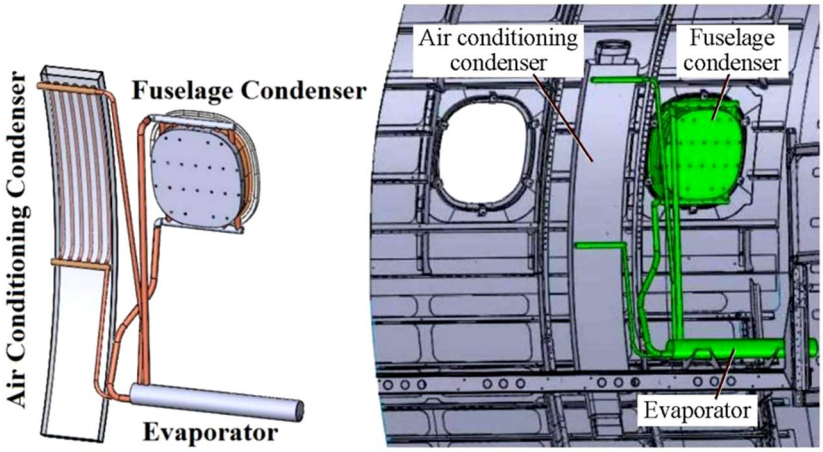

Figure 3. Thermal control system based on a loop thermosiphon with heat removal to the fuselage and dissipation into the surrounding air [11].

In aircraft with electric traction, the choice of passive thermal control systems is more relevant than in aircraft with internal combustion engines, due to the need to save electricity by eliminating coolant pumping systems and blower fans. No less important is the absence of a traditional fuel system in an electric aircraft, since fuel is the main, and sometimes the only, heat sink for heat-loaded equipment. Heat receivers in aircraft with an electric drive are the aircraft structure or the surrounding air. **Figure 3** shows a loop thermosyphon-based thermal control system, flight tested on an Embraer

aircraft [11]. The thermosyphon condensers are connected to the same evaporator by independent vapor and liquid lines. One part of the heat from the cooled object is transferred to the fuselage; the other is used for air conditioning, which must be heated to a comfortable temperature.

The A.V. Luikov Heat and Mass Transfer Institute of the National Academy of Sciences of Belarus developed heat pipes and thermosyphons for various purposes [12–14], including for cooling objects that are sources of powerful heat generation [12]. One of the latest developments is a loop thermosyphon made of aluminum, having two flat multi-channel evaporators and one condenser for cooling electronic components, developed and tested with acetone as the working fluid. In loop thermosyphons, the vapor and liquid flows are separated from each other. The coolant, as in a conventional thermosyphon, flows down from the condenser to evaporators under the action of gravity, but the absence of friction between the vapor and the liquid allows increasing the heat transfer capacity of this heat conductor. Therefore, they can be successfully used in cooling systems of electric transport power electronics. The use of aluminum as a structural material provides a significant gain in weight, which is extremely important for transport, especially aviation. A two-phase loop thermosyphon (TPLT) is a type of passive heat transfer device that has the ability to efficiently transfer heat over a long distance without any external power supply.

2. Materials and methods

2.1. Thermosyphon design

To solve the problem of increasing the efficiency of heat exchange equipment, a prototype of a loop thermosyphon was designed and manufactured, the general appearance of which is shown in **Figure 4**. The evaporator is made flat for the convenience of placing chips or other cooled elements on it. All parts of the thermosyphon are made of aluminum.

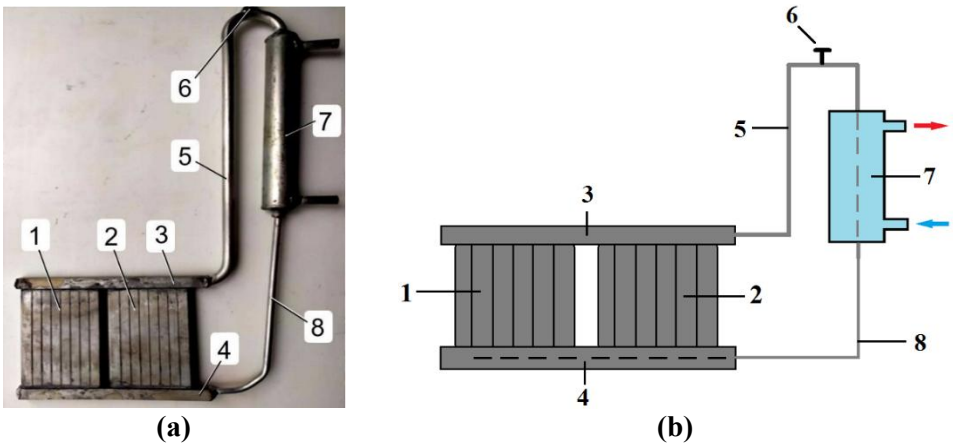

(a) **(b)**

Figure 4. Investigated double evaporator loop thermosyphon, photograph **(a)** and schematic diagram **(b)**: 1) evaporator 1; 2) evaporator 2; 3) vapor collector; 4) liquid collector; 5) vapor tube; 6) filling connection; 7) condenser; 8) liquid tube.

Table 1. Specifications of the thermosyphon (dimensions in mm).

Specifications	**Size**
Evaporator	
Number of evaporators	2
Number of mini-channels in one evaporator	8
Dimensions of one mini-channel (length × width × height)	7 × 3 × 110
Hydraulic diameter	4.2
Condenser	
Type	Tube in tube
External dimensions (length × external diameter)	200 × 24
Wall thickness	2
Vapor and liquid collectors	
Length × width × height	160 × 9 × 9
Vapor tube: $d_{in} \times L$	8 × 400
Liquid tube: $d_{in} \times L$	4 × 200

The peculiarity of the thermosyphon is the availability of two equal vertically oriented multi-channel evaporators 1 and 2, which are connected to the condenser through vapor 3 and liquid 4 collectors. The evaporators are heat receivers, each of them can have heat sources of different power (for example, chips). The heat absorbed during evaporation is transferred with the mass of vapor through the vapor outlet tube 5 to the condenser 7, which is cooled by a flow-through liquid heat exchanger. The condensate flows down to the evaporators through liquid transport tube 8. The liquid tube connects the condenser to the evaporator through the liquid collector, continues inside the liquid collector along its entire length, and evenly supplies the evaporators with working fluid. The thermosyphon condenser is equipped with a flow-through liquid heat exchanger, but heat can also be removed from the condenser of devices of this type by air convection. In this case, it is advisable to make the condenser in the form of a radiator with a developed finned heat exchange surface. All components of the thermosiphon are made of aluminum. The geometric characteristics of the thermosyphon are presented in **Table 1**.

The mini-channels in each evaporator are separated by 1 mm thick walls. The walls of the mini-channels act as internal ribs, increasing the heat exchange surface area and the evaporation rate of the working fluid. Multi-channel flat evaporator is made of extruded aluminum profile ALS-7PK70_011.1 (**Figure 5**). Wall thickness is 2 mm. The inner and outer walls of the evaporator have a smooth surface.

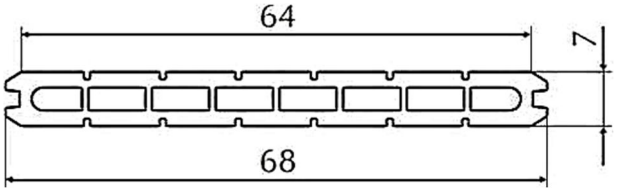

Figure 5. Cross-section of the evaporator panel.

The evaporator is made flat for the convenience of mounting the cooled elements on its surface. Tight fit of the objects of thermal regulation to the evaporator allows minimizing the contact thermal resistance. Since wetting a large area of a vertically located surface is difficult, the internal volume of the evaporator is divided into parallel channels, which improves the conditions for supplying the evaporation centers with liquid. The presence of curvilinear meniscuses formed on the walls of the channels ensures the occurrence of capillary pressure necessary for the spread of the liquid phase along the height of the channel. The division of the internal space of the evaporator into channels also helps to organize the flow and laminarize the flow of the resulting vapor, which is discharged through the vapor collector and the vapor tube into the condenser. The contribution of capillary pressure, caused by the presence of a curvilinear meniscus, to the organization of wetting of the heat exchange surface is of significant importance, since the evaporator channels have a smooth surface.

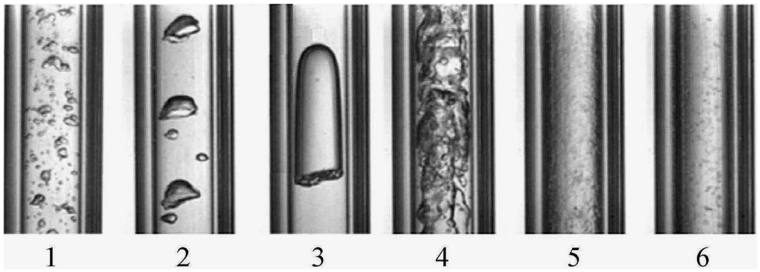

Figure 6. Changes in the two-phase flow modes in vertical mini-channels of the evaporator (d_{ch} = 4 mm) with an increase in the heat load [15]: 1) formation of mini-bubbles on the heat exchange surface; 2) merging of mini-bubbles into large clusters; 3) separation of a liquid flow into vapor plugs and liquid cuffs; 4) turbulent vapor-liquid flow; 5) stratification of a two-phase flow and formation of a thin liquid film on the wall with an accompanying increase in the vapor content in the flow; 6) flow of wet vapor.

Two-phase heat exchange during the movement of vapor-liquid mixtures through small-section channels has been considered in a number of works. Karayiannis and Mahmoud [13] conducted a study of the flow of boiling liquid in rectangular microchannels using high-speed video filming, which made it possible to examine the dependence of flow regimes on the magnitude of the heat flux supplied to the system and the relationship of the regimes with the intensity of heat transfer. In mini-channels of the heat-loaded thermosyphon evaporator, as a result of the phase transition, vapor bubbles are generated, which, with an increase in the heat flow supplied to the evaporator, grow, merge into clusters, and affect the nature of the two-phase flow. Each flow regime, from the generation of mini-bubbles on the channel wall to the flow of wet vapor, is characterized by different vapor content (**Figure 6**) [15].

The driving forces that ensure the circulation of the working fluid along the circuit of the thermosyphon are the gravitational pressure ΔP_g and the pressure ΔP_{vg}, arising as a result of the vapor generation in the annular channel of the evaporator. The operability of the thermosyphon is maintained under the condition that the combination of these driving forces exceeds or is equal to the pressure losses in the circuit:

$$\Delta P_g + \Delta P_{vg} \geq \Delta P_l + \Delta P_v + \Delta P_e + \Delta P_c \; a = 1 \quad (1)$$

where ΔP_l, ΔP_v—pressure losses in liquid and vapor tubes; ΔP_e, ΔP_c—pressure drop due to vapor generation or condensation at the liquid–vapor interface.

The internal diameter of the liquid tube is smaller than the internal diameter of the vapor tube (ratio 1:2) in order to avoid reverse vapor flow and blocking of the liquid tube.

To remove air from the thermosyphon circuit and fill it with working fluid, the device design has a filling nipple. To ensure the ability to change the filling level for research purposes, the ability to repeatedly depressurize, perform a refilling procedure, and subsequently seal the thermosyphon is provided.

2.2. Experimental equipment and experimental procedure

Heat transfer properties of the thermosyphon were determined on an experimental stand, the diagram of which is shown in **Figure 7**. The heat flow to the evaporator was supplied by means of an electric heater, which was powered by a stabilized direct current source HY10010E with a voltage setting accuracy of 1 V and a current of 0.1 A. T-type thermocouples (copper-constantan) were installed at the points of measuring the temperature of the thermosyphon components. (**Figure 8**). Thermocouple signals were recorded and analyzed by an Agilent 34980A multifunction switching and measurement unit connected to a computer. The evaporator, condenser, vapor and liquid tubes were reliably insulated to prevent heat leakage. The thermosyphon condenser is a “tube in tube” type heat exchanger and is cooled by running water coming from the LOIP FT-316-40 thermostat with a temperature maintenance accuracy of ± 0.1 °C. The temperature of the cooling water during the experiments was 20 °C.

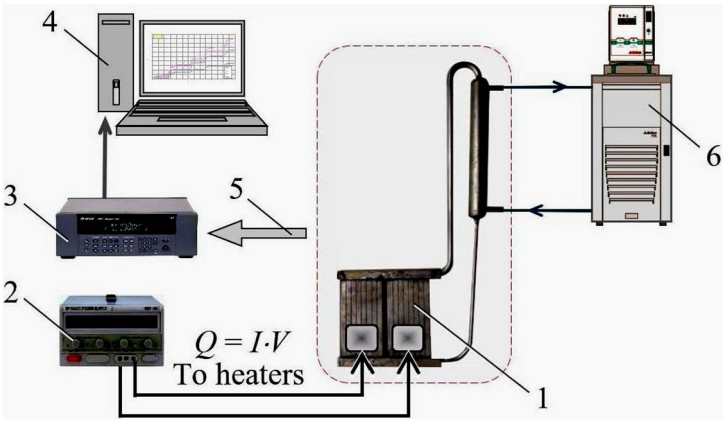

Figure 7. Schematic diagram of the experimental setup for studying the thermosyphon: 1) thermosyphon, 2) DC source, 3) Agilent, 4) computer, 5) signals from thermocouples installed on the thermosyphon, 6) thermostat.

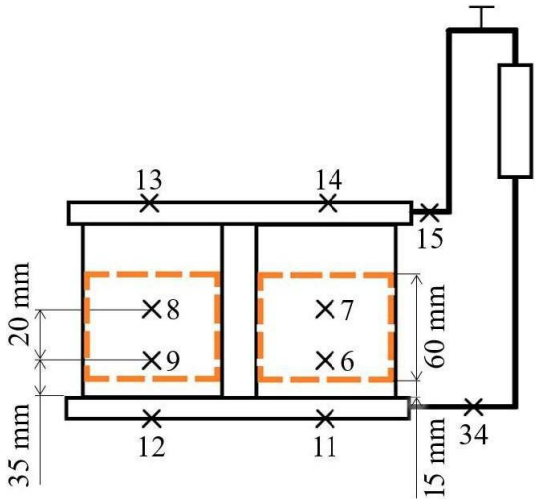

Figure 8. Arrangement of the thermocouples (×) on the evaporator panels with two heaters, condenser, vapor and liquid collectors, vapor, and liquid tubes.

Acetone, a substance of organic origin, which is a volatile liquid (dimethyl ketone, chemical formula—C_3H_6O), was used as the working fluid, the filling ratio in different experiments ranged from 15% to 63% of the evaporator volume. Acetone easily mixes with water and is characterized by low toxicity. The main properties of acetone are given in **Table 2** [16].

Table 2. Basic physical properties of acetone [16].

T_{melt}, °C	q_{melt}, kJ/kg	T_{boil}, °C	r, kJ/kg at T_{boil}	T_{cr}, °C	P_{cr}, bar	ρ_{cr}, kg/m^3
–93.2	96	56.1	524	235.0	47.6	273

The temperature distribution in the thermosyphon is determined. The thermal resistances of the evaporator (R_e), the condenser (R_c), and the entire thermosyphon (R_{TS}) at different heat powers and temperatures of the cooling medium are calculated using Equations (2)–(4):

$$R_e = \frac{\bar{T}_e - \bar{T}_v}{Q} = \frac{\frac{1}{m}\sum_{i=1}^{m} T_{e,i} - \frac{1}{n}\sum_{i=1}^{n} T_{v,i}}{Q} \quad (2)$$

$$R_c = \frac{\bar{T}_v - \bar{T}_c}{Q} = \frac{\frac{1}{n}\sum_{i=1}^{n} T_{v,i} - \frac{1}{k}\sum_{i=1}^{k} T_{c,i}}{Q} \quad (3)$$

$$R_{TS} = R_e + R_c = \frac{\bar{T}_e - \bar{T}_c}{Q} = \frac{\frac{1}{m}\sum_{i=1}^{m} T_{e,i} - \frac{1}{k}\sum_{i=1}^{k} T_{c,i}}{Q} \quad (4)$$

where $\bar{T}_e$, $\bar{T}_v$, and $\bar{T}_c$ are average values of the evaporator, vapor, and condenser temperatures, Q is the heat load.

The heat load was determined by the supplied electric power $I \times U$. Heat leakage in the wires and thermal conductivity through the thermal insulation were taken into account. Heat losses to the environment due to radiant heat exchange were estimated using Equation (5):

$$Q = \varepsilon\sigma A(T_1^4 - T_2^4) \quad (5)$$

Here $\varepsilon = 0.77$ is the coefficient of surface radiation; $\sigma = 5.67 \times 10^{-8}$ W m^{-2} K^{-4} is the Stefan-Boltzmann constant; A is the area of the radiating surface, m^2; T_1 is the average temperature of the outer surface of the thermal insulation of the thermosyphon; T_2 is the ambient temperature (room temperature).

2.3. Experiments

2.3.1. Heat loaded evaporator 1

Figure 9 illustrates the change in the temperature field in different zones of the loop thermosyphon during the experiment at a filling rate of 33% with the working fluid (acetone). Only evaporator 1 ($Q = 40$ W) is heat loaded; evaporator 2 at this stage acts as an auxiliary condenser and facilitates the rapid start of the thermosyphon. During the transition period of time 1, non-stationary heating of thermosyphon 1 occurs. The vapor is not directed into the steam tube until the saturation temperature in the steam collector reaches 60 °C.

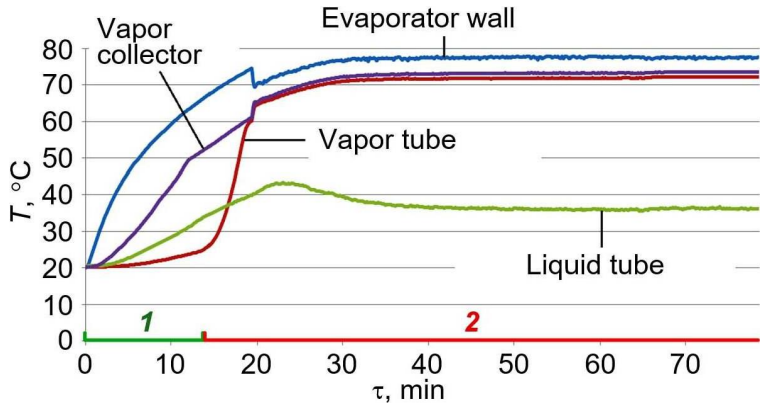

Figure 9. Temperature distribution graph during the experiment at an acetone filling rate of 33%, heat power of 40 W: 1) non-stationary process, 2) steady-state process.

After heat is supplied to evaporator 1 in the initial stage of the process (stage 1), the vapor tube heats up weakly. This indicates that this line is not filled with vapor and, therefore, the condenser is passive. It starts working after evaporator 2 is heated by the vapor condensing in its channels, which came from evaporator 1, to the saturation temperature. The steady-state operating mode of the thermosyphon is established (stage 2). A sign of completion of the transition period of the thermosyphon operation and the beginning of the stationary period is a cessation of growth and then stabilization of the temperature of the liquid phase flowing out of the condenser (**Figure 8**).

The transition from a non-stationary operating mode to a stationary one is shown in **Figure 10**. The small contour (dashed line) corresponds to the transient mode of operation of the thermosyphon (start-up mode, panel 2 acts as a condenser), the large contour (solid line) corresponds to the stationary mode of operation.

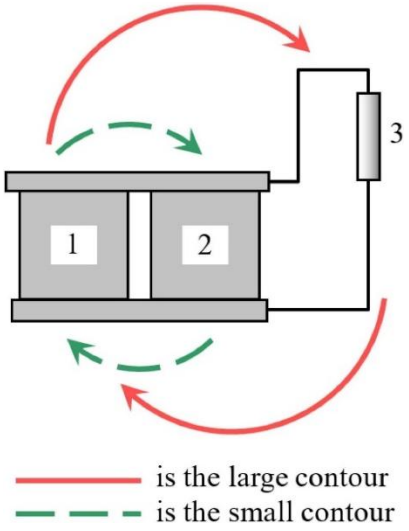

Figure 10. Two modes of operation of a thermosyphon with two evaporators: 1) evaporator 1; 2) evaporator 2; 3) condenser. The small circuit corresponds to the transient mode; the large circuit corresponds to the steady-state mode.

A Graph of temperature values of the thermosyphon components in steady-state mode (heat load supplied to panel 1) is shown in **Figure 11**.

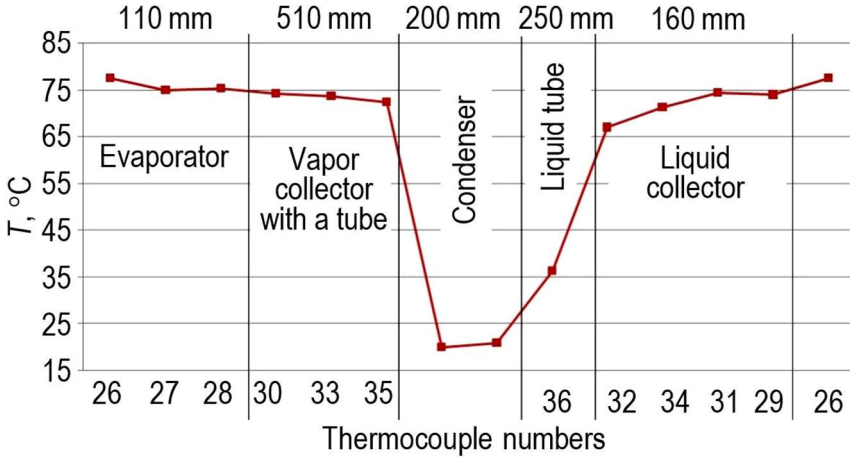

Figure 11. Temperatures of the thermosyphon components in steady-state mode.

The average value of the heat transfer coefficient in the evaporator over the phase transition surface is calculated using the Newton-Richmann equation:

$$h = \frac{Q}{A(\bar{T}_e - \bar{T}_v)} = \frac{q}{\Delta T} \tag{6}$$

Heat transfer coefficients of the evaporator 1 surface at a heat load of 40 W for different rates of filling the thermosyphon with working liquid (as a percentage in relation to the internal volume of the evaporator), is shown in **Figure 12**.

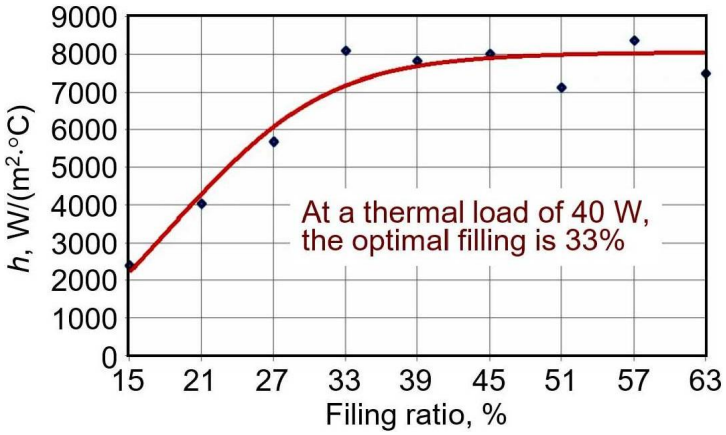

Figure 12. Effect of the degree of filling ratio with acetone on the heat transfer intensity in the evaporator, Q = 40 W.

It is evident from the graph in **Figure 12** that when the thermosyphon transfers a heat load of 40 W, significant changes in the heat transfer coefficient occur at a filling level of the evaporator with acetone up to 33%. Further increase in the rate of filling the thermosyphon with working fluid does not lead to a change in the heat transfer coefficient. Therefore, for this heat load, the optimal filling is 33%.

Important characteristics of closed two-phase thermosyphons are the total thermal resistance of the device and the thermal resistances of individual components. The graphs of the dependence of thermal resistances of the evaporator, condenser, and the entire thermosyphon (R_e, R_c, and R_{TS}), calculated using Equations (1)–(3), are shown in **Figure 13**.

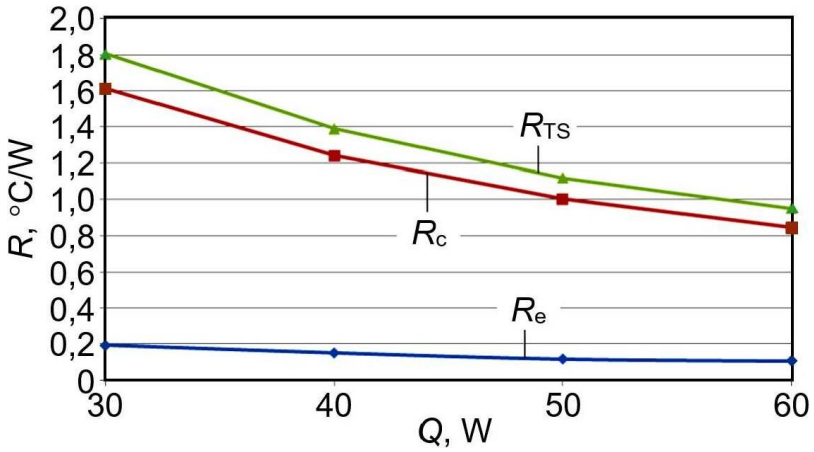

Figure 13. Dependence of thermal resistances of the evaporator (R_e), condenser (R_c), and total thermal resistance (R_{TS}) on the thermal load Q.

2.3.2. Evaporators 1 and 2 are heat loaded

A loop thermosyphon with two evaporators has the ability to receive heat from two heat sources of equal or different thermal power. To determine the behavior of the thermosiphon when a load is applied to both evaporators, the main evaporator (1) was started with a heat flow of 40 W, after reaching the steady state, a heater with a power of 20 W was connected to the additional evaporator (2). Temperature distribution data are shown in **Figure 14**. The curves in the figure indicate three stages of the process.

First, the thermosyphon is started with a heat load of 40 W on evaporator 1 (stage 1). At stage 2, the thermosyphon with the heat-loaded evaporator 1 reaches a steady-state operating mode. The third stage corresponds to the inclusion of the previously inactive evaporator 2 into operation with a heat load of 20 W and the thermosyphon reaching a steady-state mode with two heat-loaded evaporators.

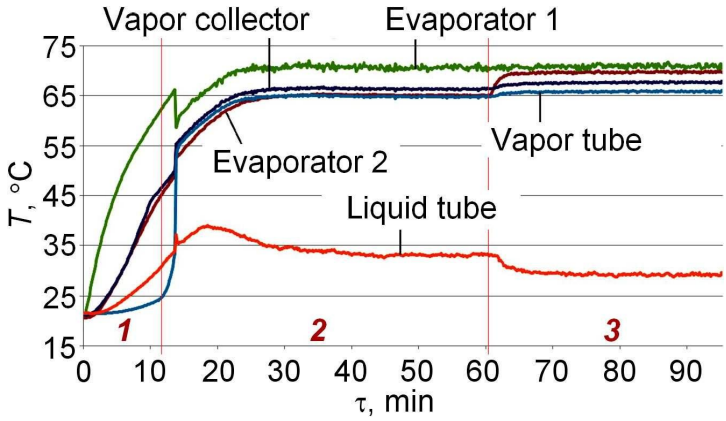

Figure 14. Temperatures of thermosyphon components with sequential switching on of evaporator 1 (40 W) and evaporator 2 (20 W).

When the heat load was applied to evaporator 2, the temperature of the main evaporator 1 remained virtually unchanged. A slight increase in the vapor temperature was observed with a noticeable cooling of the liquid phase, which is explained by the increased heat exchange in the condenser. **Figure 15** shows the temperature values on the thermosyphon body in steady-state mode with a load of 40 W on evaporator 1 and 20 W on evaporator 2. The layout of the temperature sensors on the thermosyphon is shown in **Figure 8**.

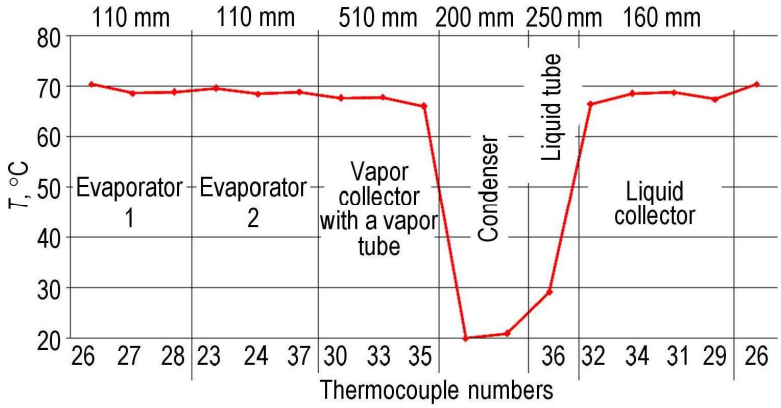

Figure 15. Temperature field along the thermosyphon in steady state with both thermosyphon evaporators active.

3. Discussion

Electric and hybrid transport allows for the reduction of the consumption of hydrocarbon fuels and improves the ecology of the planet, which is the reason for its increasing prevalence. The design of both cars and aircraft with electric power plants includes components that generate a large amount of heat during operation. This heat-

loaded equipment requires efficient and energy-saving thermal control systems. Cooling systems based on heat pipes and thermosyphons, possessing the above-mentioned qualities, have proven themselves well and require further development in connection with the growing energy intensity of electric and hybrid vehicles. A new loop thermosyphon with two evaporators and one condenser for cooling electronic components is developed and tested with acetone as the working fluid.

The results of the experimental study of the thermosyphon with two parallel panels showed that its operation is related to the difference in heating power between the two panels. The hydraulic resistance of the high-load panel is higher than the low-load panel. When there is a significant difference in the loads of the two evaporators, the high-load evaporator experiences overheating due to the insufficient fluid flow, while the low-load evaporator incurs some flow wastage. The tested thermosyphon is characterized by dynamic entry into the operating mode. Considering the importance of weight characteristics for equipment used in transport, the advantage of the thermosyphon is also its lightness, due to the choice of aluminum as a construction material.

4. Conclusions

Among the various means of temperature control of heat-loaded equipment of electric and hybrid vehicles, systems on heat pipes and thermosyphons stand out due to a number of advantages, including efficiency, simplicity, no need for energy consumption for their operation, and automatic start-up. To solve problems of optimizing the temperature conditions of operation of electronic systems, including on-board equipment of electric and hybrid transport, an aluminum loop thermosyphon was created and tested. Based on the results of the study, the following conclusions can be drawn:

1) As the transferred heat flow increases, the thermal resistance of the thermosyphon decreases, since the circulation of the working fluid along the circuit accelerates and heat exchange processes intensify. The stability of heat transfer by the thermosyphon is maintained even with non-stationary and asymmetrical heat load supplies to the evaporators.
2) An additional evaporator (2) helps to start the thermosyphon with the filling ratio 30%, acting as an auxiliary condenser during the transition mode.
3) Thermosyphons of this type can be used to create heat exchangers for passive thermal control systems for electronics, space equipment, avionics, traction drives for electric transport, etc.

Experience with aluminum shows that there are difficulties in creating effective porous structures with the required porosity, permeability and capillary potential for evaporators, since the method of their production by sintering powder particles is not applicable in this case. Modification of heat exchange surfaces can be carried out by structuring, coating with aluminum dioxide particles and other methods.

Author contributions: Conceptualization, LV and AZ; methodology, DS; software, DS; validation, LV, AZ and DS; formal analysis, AZ; investigation, DS; resources, LV; data curation, DS; writing—original draft preparation, AZ; writing—review and

editing, AZ; supervision, LV; project administration, LV. All authors have read and agreed to the published version of the manuscript.

Funding: This research was funded by the Belarusian Republican Foundation for Fundamental Research, grant No. T23RNF-227.

Conflict of interest: The authors declare no conflict of interest.

References

1. Kendall K. Low carbon integrated vehicles and buildings. Mechanical Engineering Advances. 2024; 2(1). doi: 10.59400/mea.v2i1.282
2. Ekici F, Orhan G, Gümüş Ö, et al. A policy on the externality problem and solution suggestions in air transportation: The environment and sustainability. Energy. 2022; 258: 124827. doi: 10.1016/j.energy.2022.124827
3. Gan Y, Wang M, Lu Z, et al. Taking into account greenhouse gas emissions of electric vehicles for transportation de-carbonization. Energy Policy. 2021; 155: 112353. doi: 10.1016/j.enpol.2021.112353
4. Sanguesa JA, Torres-Sanz V, Garrido P, et al. A Review on Electric Vehicles: Technologies and Challenges. Smart Cities. 2021; 4(1): 372-404. doi: 10.3390/smartcities4010022
5. Andersen PH, Mathews JA, Rask M. Integrating private transport into renewable energy policy: The strategy of creating intelligent recharging grids for electric vehicles. Energy Policy. 2009; 37(7): 2481-2486. doi: 10.1016/j.enpol.2009.03.032
6. Coutinho M, Afonso F, Souza A, et al. A Study on Thermal Management Systems for Hybrid–Electric Aircraft. Aerospace. 2023; 10(9): 745. doi: 10.3390/aerospace10090745
7. Xie Y, Savvarisal A, Tsourdos A, et al. Review of hybrid electric powered aircraft, its conceptual design and energy management methodologies. Chinese Journal of Aeronautics. 2021; 34(4): 432-450. doi: 10.1016/j.cja.2020.07.017
8. Justin CY, Payan AP, Briceno SI, et al. Power optimized battery swap and recharge strategies for electric aircraft operations. Transportation Research Part C: Emerging Technologies. 2020; 115: 102605. doi: 10.1016/j.trc.2020.02.027
9. Tom L, Khowja M, Vakil G, et al. Commercial Aircraft Electrification—Current State and Future Scope. Energies. 2021; 14(24): 8381. doi: 10.3390/en14248381
10. Asli M, König P, Sharma D, et al. Thermal management challenges in hybrid-electric propulsion aircraft. Progress in Aerospace Sciences. 2024; 144: 100967. doi: 10.1016/j.paerosci.2023.100967
11. Oliveira JLG, Tecchio C, Paiva KV, et al. In-flight testing of loop thermosyphons for aircraft cooling. Applied Thermal Engineering. 2016; 98: 144-156. doi: 10.1016/j.applthermaleng.2015.12.008
12. Vasiliev L, Zhuravlyov A, Kuzmich M, et al. Development and testing of a novel horizontal loop thermosyphon as a kW-class heat transfer device. Applied Thermal Engineering. 2022; 200: 117682. doi: 10.1016/j.applthermaleng.2021.117682
13. Vasiliev LL, Zhuravlyov AS. Two-phase heat transfer devices for passive cooling of electric and hybrid aircraft onboard equipment. International Journal of Sustainable Aviation. 2023; 9(2): 89. doi: 10.1504/ijsa.2023.129938
14. Vasiliev LL, Zhuravlyov AS, Kuz′mich MA, et al. Loop Thermosyphon for Cooling Heat-Loaded Electronics Components. Journal of Engineering Physics and Thermophysics. 2023; 96(7): 1708-1715. doi: 10.1007/s10891-023-02840-8
15. Karayiannis TG, Mahmoud MM. Flow boiling in microchannels: Fundamentals and applications. Applied Thermal Engineering. 2017; 115: 1372-1397. doi: 10.1016/j.applthermaleng.2016.08.063
16. Vargaftik NB, Vinogradov YK, Yargin VS. Handbook of physical Properties of Liquids and Gases. Pure Substances and Mixures, 3rd ed. Begel House, Inc., New York, Wallingford (UK); 1996.